Laser Forming of Ti-6Al-4V: Research Overview

P.A. Kobryn and S.L. Semiatin

Air Force Research Laboratory, AFRL/MLLM, Building 655, Suite 1
Wright-Patterson Air Force Base, OH 45433-7817

Abstract

Laser forming is a solid-freeform-fabrication process which is being investigated for titanium-component manufacturing based on its cost-reduction potential. However, before it can be transitioned to production, the relationships between processing parameters, input materials, and deposit properties must be understood. In the present work, efforts were undertaken to characterize these relationships. These efforts included a comparison of different laser-forming processes, an investigation of the effect of processing parameters on deposit structure, determination of microstructure evolution via laser-processing experiments and thermal FEM modeling, and a study of texture/microtexture evolution. An overview of the results of this laser-forming research are provided in this paper.

Introduction

Laser forming is a solid-freeform-fabrication method which can be used to manufacture solid metallic components directly from CAD files. During laser forming, powder is fed into a melt pool which is produced by a sharply-focused laser beam. Parts are built in a layer-by-layer fashion by rastering the laser and powder source across the substrate. Laser forming has many potential applications, including production of functional prototypes, short-run component fabrication, component repair, and fabrication of functionally-graded materials.

Currently there are two main types of laser-forming systems: those using relatively low-power, small-spot-size Nd-YAG lasers and those using relatively high-power, large-spot-size CO_2 lasers. The Nd-YAG-laser systems typically have maximum powers of 500 to 1200W, circular beam cross-sections, and gaussian intensity distributions. The CO_2 systems have maximum powers of up to 18kW with varying beam cross-sections and intensity distributions. In general, the Nd-YAG systems deposit lines up to ~1 mm in width, while the CO_2 systems deposit lines up to ~15 mm in width. The smaller-spot-size systems generally have lower powder-use efficiencies and deposition rates but more precise shape-making capabilities.

Laser forming is particularly attractive for the fabrication of titanium aerospace components because it can greatly reduce the buy-to-fly ratio and lead time for production, two factors which impact cost. Thus, a number of recent efforts have been undertaken to develop titanium laser-forming processes [1,2,3,4]. Much of the focus of this prior research has been on equipment development and mechanical property measurements [1,2]. Acceptable processing parameters have been determined largely through trial-and-error approaches. On the other hand, only limited work has been done to establish the relationship between process parameters and the structure of deposits [3,4]. Such an understanding is critical for both process control and process design.

The work reported here is part of a larger effort to establish the effect of process parameters and input materials on deposit structure, texture, and mechanical properties, and is divided into the following four thrusts: Comparison of Various Processes, Effect of Process Parameters on Deposit Structure, Phenomenological Modeling of Microstructure Evolution, and Texture/Microtexture Evolution.

Materials and Procedures

Materials: The materials used in this investigation consisted of one lot of gas-atomized prealloyed Ti-6Al-4V powder made by Crucible Research and two lots of hot-rolled Ti-6Al-4V plate, each having an equiaxed alpha microstructure. The powder had a composition (in weight percent) of 6.29 aluminum, 3.93 vanadium, 0.099 oxygen, 0.0059 hydrogen, 0.009 nitrogen, 0.042 carbon, 0.041 iron, balance titanium and mesh size of -100, +325 (particle sizes between 45 and 150 μm). The thinner Ti-6Al-4V plate (2.90-mm thick) had a composition (in weight percent) of 6.31 aluminum, 4.15 vanadium, 0.12 oxygen, 0.0052 hydrogen, 0.01 nitrogen, 0.02 carbon, 0.21 iron, balance titanium. The thicker plate (13.23-mm thick) had a composition (in weight percent) of 6.19 aluminum, 3.89 vanadium, 0.20 oxygen, 0.0074 hydrogen, 0.01 nitrogen, 0.02 carbon, 0.12 iron, balance titanium. Prior to deposition, the plates were lapped on both sides to a surface finish of 12 to 14 μm and degreased using acetone and alcohol.

Comparison of Various Processes. In preliminary work to establish the structures which evolve during laser forming, Ti-6Al-4V deposits of various sizes and shapes were made using three laser-forming systems: Optomec Design Co.'s LENS™ system, Los Alamos National Lab's DLF system, and the system at the Applied Research Laboratory (ARL) at The Pennsylvania State University. The LENS™ and DLF systems use ~500W (maximum power) Nd:YAG lasers with ~1-mm-diameter circular beams with gaussian intensity distributions, while the ARL system uses a 14kW (maximum power) CO_2 laser with a ~13-mm-wide square beam with a uniform intensity distribution. All of the deposits were made using the processing parameters recommended by the operators of the given system. Polished and etched cross-sections were examined using optical microscopy. The grain morphology, grain size, and microstructure were determined, and a comparison of the results from the various systems was made.

Effect of Process Parameters on Deposit Structure. A detailed investigation of the effect of power, traverse speed, and substrate thickness was performed using the LENS™ system [4]. For this investigation, eleven deposits, each 12 mm x 24 mm x 4 layers, were made on both the thin and thick Ti-6Al-4V substrates using various combinations of laser power and traverse speed. The selected deposition conditions represented the optimal parameters suggested by the manufacturer of the LENS™ system, conditions 20 percent below and above the optimal-parameter specification, and selected additional combinations in which the power was set slightly above or below the ±20 percent range. Polished and etched cross-sections of all of the deposits were examined using optical microscopy and the effect of the variables on deposit characteristics such as grain size, porosity, and build height was assessed.

Phenomenological Modeling of Microstructure Evolution. To gain insight into the evolution of macrostructure during laser forming of Ti-6Al-4V, a combination of experimental measurements

and estimates, finite-element-method (FEM) modeling results, and a previously determined solidification map for Ti-6Al-4V [5] was used. Due to the complexity of the laser-forming process, the laser-glazing process was used for this initial effort. To this end, the LENS and ARL systems were used (without powder) to make single-line laser-glaze passes over Ti-6Al-4V substrates at various combinations of power and traverse speed. The resulting glazes were sectioned perpendicular to the direction of laser travel and metallographically prepared. The size and shape of the fusion and heat-affected zones and the grain morphology in the fusion zone were characterized.

Thermal FEM simulations of various laser glazes were performed using the ProCAST™ solidification modeling package from UES, Inc. [6] and the thermophysical properties of the substrate [7]. The FEM-predicted sizes and shapes of the fusion and heat-affect zones were compared to the measured sizes and shapes. If a suitable match was obtained, the FEM-predicted thermal gradients and solidification rates were plotted on the Ti-6Al-4V solidification map. The predicted laser-glaze grain morphology was then compared to the actual laser-glaze grain morphology. The results were used to draw conclusions about the two laser-forming systems.

Texture/Microtexture Evolution. To determine the effect of substrate texture on deposit texture, a combination of x-ray diffraction (XRD) [8] and orientation imaging microscopy (OIM) [9] techniques were used to determine the texture of the thicker substrate and the corresponding LENS™ deposit. Both α- and β-phase textures of the substrate in the as-received condition and the α-phase texture of the substrate in the β-annealed condition were measured via XRD, while the α-phase texture of the substrate and the deposit in the sub-transus heat-treated condition were measured via OIM. The resulting inverse pole figures (IPFs) for the in-plane (x,y) and substrate-normal (z) directions were compared, and preliminary conclusions regarding the effect of substrate texture on deposit texture were drawn.

Results

Comparison of Various Processes. The macrostructures of the LENS™, DLF, and ARL deposits were columnar (Figure 1a,b,c) with average grain widths of 120, 115, and 750 μm, respectively. The columnar grains in longitudinal cross-sections of the LENS™ deposits oscillated back and forth from the substrate to the surface of the deposit, those in the DLF deposits grew at a single acute angle from the substrate, and those in the ARL deposits grew perpendicularly to the substrate. The angled growth of the columnar grains (or lack thereof) was likely due to the effect of laser travel on the direction of heat removal. In the LENS™ and DLF systems, the heat flow direction was affected by the laser movement, while in the ARL deposits it was not.

The microstructures of the LENS™ and DLF deposits were very similar (Figure 1d,e). These microstructures were fine Widmanstätten in nature with very fine equiaxed alpha particles distributed both within the grains and along the grain boundaries, indicating that the cooling rate after solidification was very high. The microstructures of the ARL deposits were much coarser. The internal grain structure was primarily Widmanstätten in nature with occasional small alpha colonies along the grain boundaries (Figure 1f). Continuous grain-boundary alpha was also found along some grain boundaries, indicating a somewhat slower cooling rate.

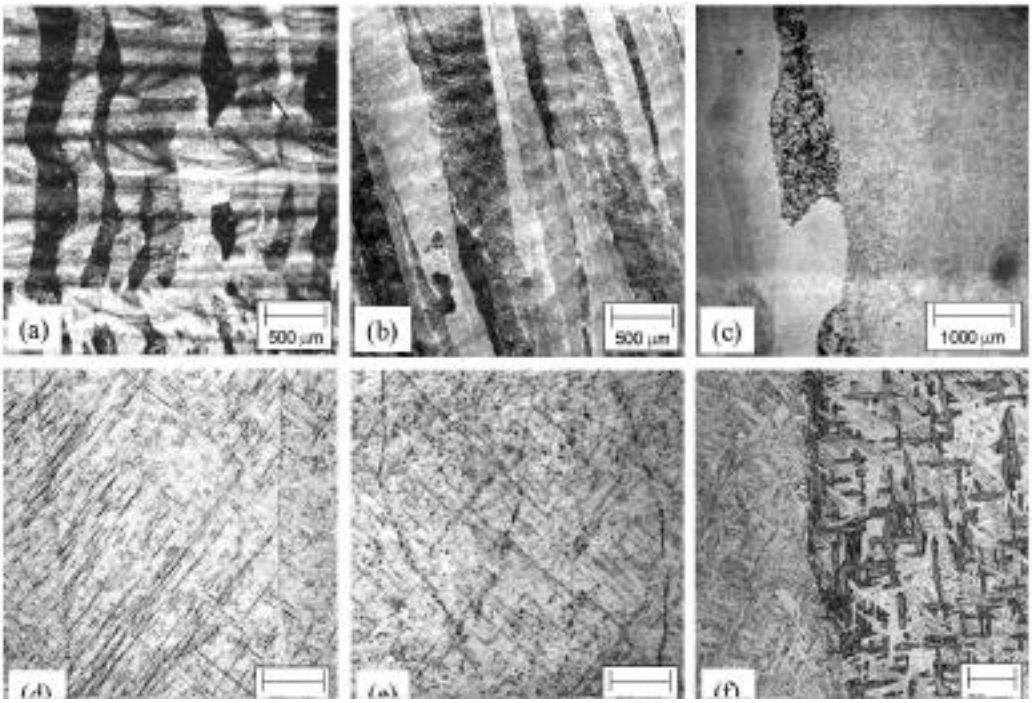

Figure 1. Macrostructures (a-c) and microstructures (d-f) of LENS™, DLF, and ARL Ti-6Al-4V laser deposits, respectively.

Effect of Process Parameters on Deposit Structure. The results of the detailed investigation of the effect of power and traverse speed on deposit structure are best presented graphically (Figure 2). The grain width decreased with increasing traverse speed (Figure 2a,b), but was largely unaffected by power level. The thin-substrate and thick-substrate grain-width data exhibited nearly identical trends with large but similar variability. Porosity tended to decrease with increasing traverse speed *and* increasing power (Figure 2c,d). Porosity was found to depend on substrate thickness also, as lack-of-fusion porosity occurred more frequently and in larger amounts in thin-substrate deposits. Build height tended to decrease as traverse speed increased, but no clear relationship between laser power and build height was found (Figure 2e,f). Substrate thickness also affected build height. In general, the thin-substrate deposits were thicker and had a larger variability than the thick-substrate deposits. This trend was attributed to the increased amount of porosity in the thin-substrate deposits [4].

Phenomenological Modeling of Microstructure Evolution. As expected, the laser glazes from the LENS™ and ARL systems were markedly different in size and shape. The fusion and heat-affected zones in the LENS™ glazes were roughly semi-circular in shape, 1 to 2 mm in width, and 0.4 to 0.9 mm in depth. The fusion and heat-affected zones in the ARL glazes were roughly semi-elliptical in shape, 13 to 18 mm in width, and 2.5 to 8 mm in depth. The grain morphology in the fusion zones of the LENS™ glazes was clearly columnar, while that in the fusion zones of the ARL glazes was somewhat mixed in nature (Figure 3a,b).

The FEM simulations predicted similar fusion and heat-affected zone sizes and shapes to those observed in the actual glazes (Figure 3c-f). The depths of the fusion zones were predicted very accurately, while the predicted heat-affected-zone depths were qualitatively accurate. Hence, the simulation results were concluded to be reasonable and the resulting thermal gradient

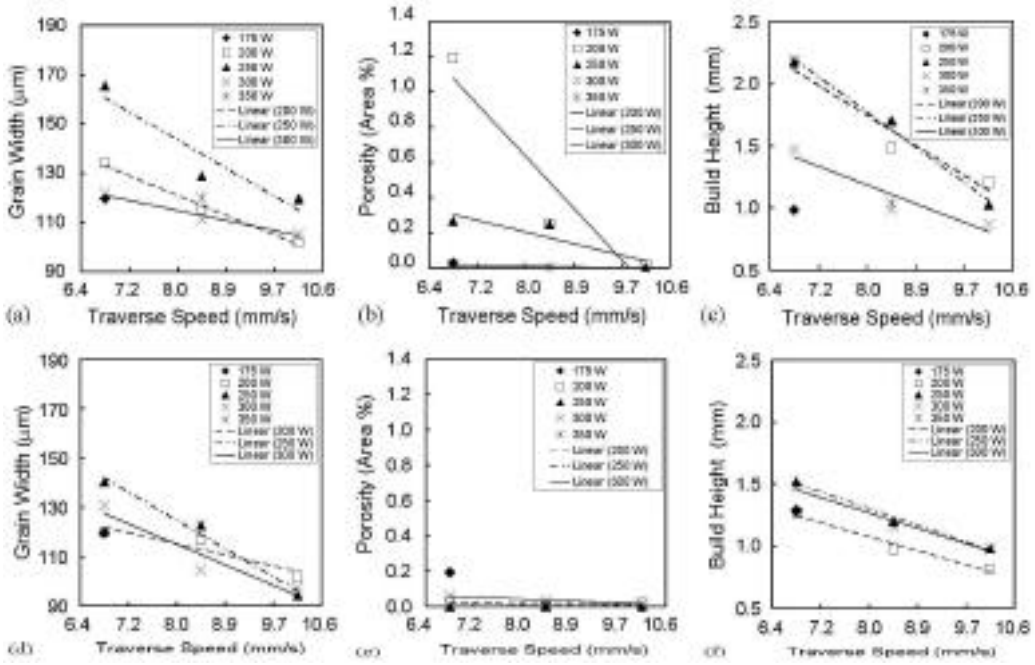

Figure 2. Grain width, porosity, and build height as a function of traverse speed for thin substrates (a-c) and thick substrates (d-e).

and solidification rate predictions were plotted on the Ti-6Al-4V solidification map (Figure 4). The map indicated that the expected morphology for the LENS™ glaze is columnar and for the ARL glaze is mixed. Because these were the observed morphologies, the solidification map was concluded to be a viable tool for assessing the grain morphology of laser-processed solidification products.

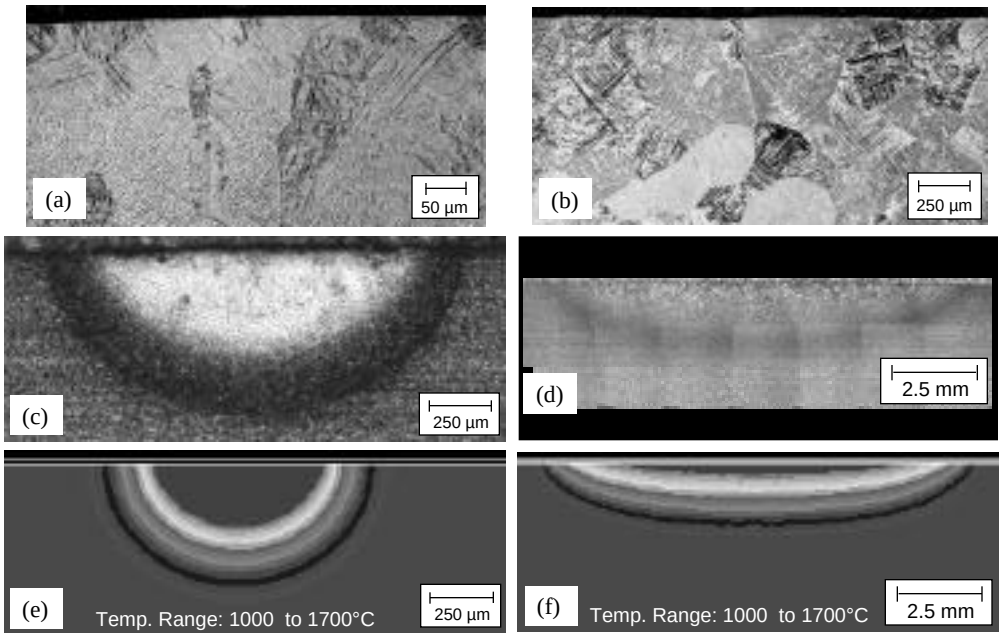

Figure 3. Actual macrostructures and fusion/heat-affected zones and the corresponding FEM-predicted fusion/heat-affected zones for LENS™ (a,c,e) and ARL (b,d,f) laser glazes.

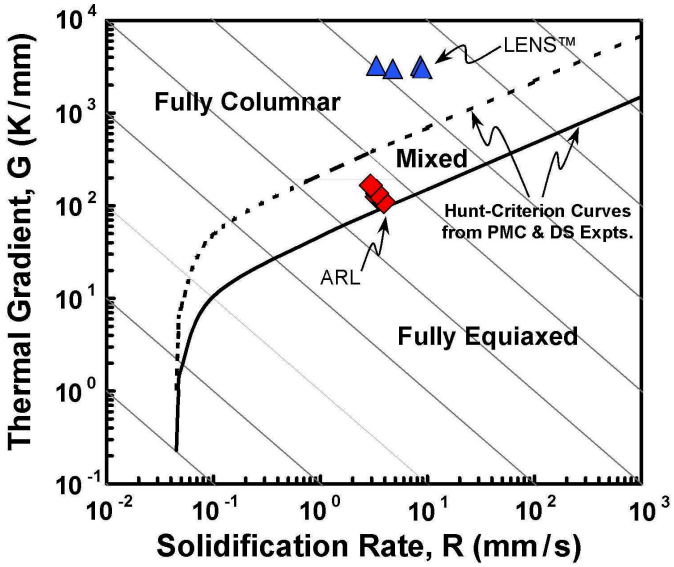

Figure 4. Ti-6Al-4V solidification map with simulated laser-glaze data points.

Texture/Microtexture Evolution. Because the surface of the substrate melts during laser forming, the volume of material just below the melted layer must reach a temperature above the β-transus temperature. Hence, if epitaxial growth from the solid substrate was to occur, the β-*phase* texture of the deposit would be related to the β-*phase* texture of the substrate. However, the subsequent β → α + β transformation eliminates much of the original β phase, making it very difficult to assess the original β-phase texture.

The α-phase texture of the substrate in the as-received condition was different from that in the β-annealed condition, which was expected based on the substrate's processing history. Additionally, the [00·2] α-phase pole figure from the β-annealed substrate did not correspond directly to the [110] β-phase pole figure from the as-received substrate. This partial correspondence indicated that the β phase which formed upon heating during β annealing likely did not grow epitaxially from the existing β alone, but also nucleated independently within the α. Hence, the as-received β-phase texture could not be used as an estimate of the β-phase texture at temperatures within the β phase field, and therefore could not be used to draw conclusions about the relationship between the substrate and deposit textures. Instead, the α-phase texture of the deposit had to be compared to the α-phase texture of the β-*annealed* substrate.

This comparison yielded interesting results (Figure 5). The y-direction IPFs showed very good agreement, while the x- and z-direction IPFs did not. One possible source of the partial disagreement was the fact that only a small number of grains was sampled during OIM of the deposit, resulting in incomplete texture representation. Another possible source was texture caused by the preferred growth direction during solidification. Because solidifying cubic crystals grow fastest in the <100> direction [10], solidification structures tend to develop <100> fiber textures in the direction of columnar grain growth. Hence, the deposit might have developed a <100> fiber texture in the z direction during solidification (in the β phase).

To determine if a fiber texture had indeed formed in the deposit, the z-direction α-phase IPF for material with a sharp <100> β-phase fiber texture was constructed based on the burgers relationship for the β → α transformation. The resulting IPF shared many features with the z-direction IPF from the deposit, indicating that solidification played a strong role in deposit texture evolution (Figure 6). Thus, deposit texture was concluded to be related to both the substrate texture and solidification texture.

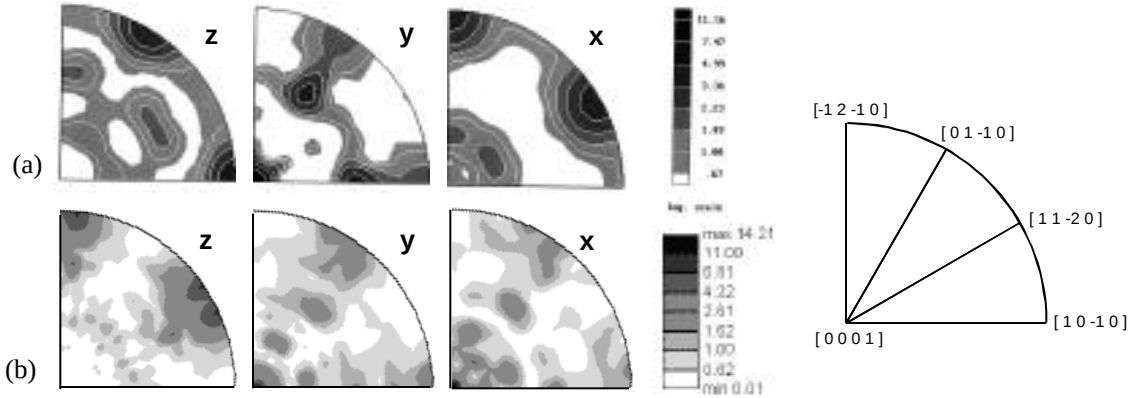

Figure 5. IPFs illustrating the α-phase texture of (a) β-annealed substrate and (b) LENS™ deposit.

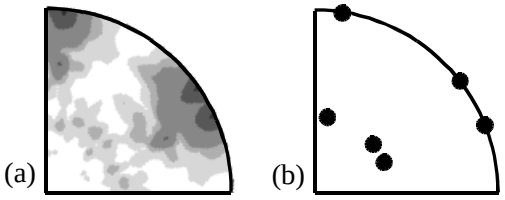

Figure 6. (a) Substrate-normal direction IPF for the α phase of a LENS™ deposit, and (b) the expected α-phase IPF for the columnar growth direction assuming random orientation of nuclei.

Summary and Conclusions

The effect of process variables and input materials on structure and texture of laser-deposited Ti-6Al-4V was established using a combination of laser-deposition experiments, FEM and phenomenological modeling, and texture analysis techniques. From this work, the following conclusions were drawn:

1. Laser forming of Ti-6Al-4V can be performed over a wide range of processing conditions and typically results in columnar macrostructures and fine to very fine transformed microstructures.

2. The width of the columnar grains decreases with increasing cooling rates associated with high traverse speeds and is not substantially affected by substrate thickness.

3. Porosity decreases with increasing traverse speed and power level, and is more prevalent when thin substrates are used.

4. The overall build height decreases with increasing speed, but the influence of power level is not straightforward. Lack-of-fusion porosity can greatly affect solidification conditions and the resulting build height during laser deposition.

5. Thermal FEM modeling and the Ti-6Al-4V solidification map are useful tools for predicting the grain morphology in laser glazes.

6. Deposit texture evolution is affected by both the substrate texture and the solidification process.

Acknowledgements

This work was conducted as part of the in-house research activities of the Processing Science Group of the Air Force Research Laboratory's Materials and Manufacturing Directorate. The support and encouragement of the Laboratory management and the Air Force Office of Scientific Research (Dr. C.S. Hartley, program manager) are gratefully acknowledged. The assistance of various personnel at Optomec Design Co., the Materials Science and Technology Division at Los Alamos National Laboratory, and the High Energy Processing Department at The Applied Research Laboratory at The Pennsylvania State University in fabricating the deposits, M. Luce, B. Lewis, and S. Apt in preparing the metallographic specimens, Lambda Research in performing the x-ray diffraction analysis, and T. Bieler in performing the OIM analysis is also much appreciated.

References

[1] Schriempf, J. T., Whitney, E.J., Blomquist, P.A., Arcella, F.G., *Advances in Powder Metallurgy and Particulate Materials*, v. 3, Princeton, NJ: Metal Powder Industries Federation, 1997:21-51.
[2] Keicher D.M., Miller, W.D., *Hard Coatings Based on Borides, Conference: Carbides & Nitrides: Synthesis, Characterization & Applications*, San Antonio, TX, USA, 16-19 Feb. 1998, Warrendale, PA: TMS, 1998:369.
[3] Brice, C.A., Schwendner, K.I., Mahaffey, D.W., Moore, E.H., Fraser, H.L., *Proceedings of the 10th Solid Freeform Fabrication Symposium*, University of Texas at Austin, Austin, TX, USA, Aug. 1999.
[4] Kobryn, P.A., Moore, E.H., and Semiatin, S.L., *Scripta Materialia*, v. 43, no. 4, 2000.
[5] Kobryn, P.A. and Semiatin, S.L., AFRL Materials & Manufacturing Directorate, WPAFB, OH, unpublished research, 1999.
[6] *ProCAST™ Users Manual & Technical Reference*, Version 3.1.0, UES Software, Inc., Dayton, OH, 1998.
[7] Henderson, J.B. and Groot, H., *Technical Report No. TPRL 1284*, Thermophysical Properties Research Laboratory, Purdue University, West Lafayette, IN, 1993.
[8] Kocks, U.F., Tome, C.N., and Wenk, H.-R., *Texture and Anisotropy*, Cambridge, 1998.
[9] Adams, B.L., Wright, S.I., and Kunze, K., *Metall. Trans. A*, v. 24A, 1993:819-831.
[10] Flemings, M.C., *Solidification Processing*, McGraw-Hill, 1974: 159-160.